

Comparison of vegetation succession patterns in the monsoon and arid regions of northern China over the past two centuries: Implications for ecosystem restoration projects

Jiaqi Pang^a, Guoqiang Ding^{a,b,*}, Panpan Ji^a, Yuanhao Sun^a, Chuanyi Duan^a, Yu Cao^a, Jiheng Shi^a, Ruijin Chen^a, Jianhui Chen^{a,*}

^a MOE Key Laboratory of Western China's Environmental System, College of Earth and Environmental Sciences, Lanzhou University, Lanzhou 730000, PR China

^b Key Laboratory for Semi-Arid Climate Change of the Ministry of Education, College of Atmospheric Sciences, Lanzhou University, Lanzhou 730000, PR China

ARTICLE INFO

Editor: Howard Falcon-Lang

Keywords:

Pollen
Vegetation succession
Northern China
Terrestrial ecosystems
Human–environment interaction

ABSTRACT

Understanding vegetation responses to climatic and anthropogenic changes is important for predicting future ecosystem trajectories and informing restoration projects in northern China. In this paper, we report high-resolution pollen records from Lake Gonghai (monsoon region) and Lake Yueliang (arid region) to investigate the relationship between vegetation, climate, and human activity over the past two centuries. Prior to 1900 CE, Lake Gonghai supported abundant arboreal vegetation under humid conditions, with extensive pastoralism indicated by high coprophilous fungal spores. During 1900–1960 CE, increasing aridity and social instability led to vegetation degradation and reduced pastoral intensity. After 1960 CE, ecological restoration policies promoted vegetation recovery, accompanied by a shift from pastoralism to *Hippophae*-dominated cultivation. In contrast, vegetation succession at Lake Yueliang has remained primarily climate-driven. Before 1900 CE, *Artemisia*–*Tamarix* desert–steppe communities prevailed under relatively humid conditions. During 1910–1990 CE, rising aridity induced a transition toward *Amaranthaceae*–*Nitraria* communities. After 1990 CE, persistent drought stabilized xerophytic vegetation composition. We suggest that vegetation dynamics across a large spatial scale have been (1) more strongly influenced by human activities in the monsoon region, with anthropogenic impacts intensifying since 1960 CE, and (2) primarily driven by climate in the arid region, with a west-to-east transition from warming-wetting to warming-drying. Our findings emphasize divergent regional ecosystem trajectories and the need for restoration strategies tailored to distinct climatic and anthropogenic contexts in northern China.

1. Introduction

Amid accelerating global warming and intensified human activities, ecological and environmental issues such as frequent extreme weather events, biodiversity loss, and escalating pollution have become increasingly severe. The Earth system and human development face unprecedented challenges, and the sustainable human–environment interactions have become a central focus in ecological research (IPCC, 2021, 2023). Terrestrial ecosystems play a crucial role in biogeochemical cycles, species diversity, climate regulation, and hydrological cycles, and are essential for addressing global environmental change and promoting sustainable development (Chapin et al., 2002). Vegetation, as

a critical component of terrestrial ecosystems, is dynamically influenced by both climate change and human activities (Piao et al., 2018; Zhao et al., 2021; Zhou S et al., 2023; Zou et al., 2025). On one hand, temperature rises and precipitation changes caused by global warming have significantly impacted vegetation structure and distribution (Berdugo et al., 2022; Fu et al., 2015; Wang Y et al., 2024). On the other hand, the implementation of ecological restoration projects (Yue et al., 2024; Zhang et al., 2024), changes in land use patterns (Theuerkauf et al., 2015; Wang C et al., 2024), pastoral activities (Batunacun Wieland et al., 2021; Hanke et al., 2014), and urbanization processes (García-Mozo et al., 2016; Zhang Z et al., 2023a) also contribute to vegetation changes. However, current assessments of vegetation dynamics primarily rely on

* Corresponding authors at: MOE Key Laboratory of Western China's Environmental System, College of Earth and Environmental Sciences, Lanzhou University, Lanzhou 730000, PR China.

E-mail addresses: dqq@lzu.edu.cn (G. Ding), jhchen@lzu.edu.cn (J. Chen).

satellite-based remote sensing data, which typically cover relatively short periods (less than 50 years) and mainly focuses on periods when vegetation has undergone significant changes due to human interference, making it difficult to trace vegetation states and environmental changes from historical periods (Zeng et al., 2022; Zhang Z et al., 2023b). Therefore, obtaining long-term, reliable evidence of vegetation change and understanding the evolutionary trajectories and driving mechanisms of these shifts are crucial for addressing global climate change and advancing ecological restoration efforts.

Pollen records in lake sediments serve as a crucial proxy for Quaternary environmental reconstruction. Their assemblages preserve comprehensive records of the species composition, abundance, and diversity of historical plant communities, thereby providing high-resolution archives for investigating long-term vegetation succession and its driving mechanisms (Stegner and Spanbauer, 2023; Xu et al., 2024). With the aid of proxies such as pollen, there has been a relatively systematic understanding of Holocene vegetation succession patterns in China (Ding et al., 2022; Sun et al., 2022; Wang et al., 2025; Zhao et al., 2024). However, compared to long-term studies, research on vegetation change over the past two centuries during the Anthropocene remains relatively limited. Existing pollen records indicate that vegetation changes over the past two centuries may have deviated from the natural evolutionary trajectory, with anthropogenic forcing becoming the main driving factor (Poraj-Górska et al., 2017; Rodríguez-Zorro et al., 2015; Xiao et al., 2013). For instance, pollen records from lakes in the Yangtze River Basin and Northeast China indicate a decline in tree pollen (such as *Pinus*), while pollen from anthropogenic plants (such as cereals, crucifers and Urticaceae) and pioneer plants (such as *Betula* and *Populus*) has increased (Ge et al., 2018, 2021; Han et al., 2021; Lv et al., 2024; Mackenzie et al., 2018). This coordinated change may reflect extensive deforestation, land reclamation, and agricultural expansion. In contrast, pollen assemblages from lakes in the northeastern Tibetan Plateau and eastern Xinjiang primarily reflect the transition of regional vegetation landscapes, with an increase in *Artemisia* and other grassland plants potentially responding to improved regional moisture conditions (Ren et al., 2020; Zhao et al., 2008). These findings suggest that vegetation responses to climatic changes and human activities over the past two centuries may exhibit significant spatial heterogeneity across different regions. However, current research faces two key limitations. First, limited cross-regional comparisons hinder our understanding of spatial patterns in vegetation succession. Second, the timing of the transition from climate-driven to human-driven vegetation dynamics and the regional variability in response mechanisms remain poorly constrained, highlighting the need for integrated multi-regional investigations.

The past two centuries represent a critical transitional period in Earth's history, providing a unique context for studying human–environment relationships. This period is characterized not only by a rate of global warming that exceeded geological historical norms (McCulloch et al., 2024) but also by the unprecedented intensity of human activities. Since the Industrial Revolution, land-use change and fossil fuel combustion have gradually become the dominant drivers of environmental change (Zalasiewicz et al., 2021). Distinct climatic transitions, such as the end of the Little Ice Age and the accelerated warming since the mid-20th century, together with transformative historical events such as the “Great Acceleration” (Steffen et al., 2015), have profoundly altered the structure and function of global ecosystems. The combined influence of extreme anthropogenic forcing, distinctive climatic variability, and transformative historical events makes this period a critical temporal window for understanding human–environment interactions. However, research on terrestrial ecosystem changes during this phase remains limited. Most existing studies focus on single sites or localized areas and lack regional-scale comparative analyses. The monsoon and arid regions of China exhibit significant spatial heterogeneity in terms of climate regimes and social development (Chen et al., 2024). The monsoon region is governed by the East Asian summer monsoon circulation, characterized by synchronous rainfall and heat,

alongside a high concentration of population and economic activity. The arid region is primarily governed by the mid-latitude westerlies, with scarce and unevenly distributed precipitation. Its eastern edge is affected by monsoon systems, forming a transitional zone. The overall socioeconomic development level in this region is relatively low. These climatic and socioeconomic differences not only lead to different vegetation responses to climate and human activities in the two regions, but also complicate the interactions among climate change, vegetation distribution, and land-use changes (Cao et al., 2022). Consequently, there is an urgent need to investigate vegetation–climate–human activity relationships to comprehensively reveal the differences in vegetation responses of the northern Chinese land ecosystems over the past two centuries under different climatic backgrounds and human activity intensities.

To better understand the regional differences and driving mechanisms of vegetation succession in northern China over the past two centuries, we selected Lake Gonghai (the monsoon region) and Lake Yueliang (the arid region) as representative study areas (Fig. 1). The vegetation types and land use patterns in the watersheds of these two lakes differ significantly, each representing the overall environmental characteristics of their respective regions. The climatic environments and human activities over the past two centuries in both regions were reconstructed through analyses of pollen and coprophilous fungal spore records, combined with other proxy indicators, historical documents, and socioeconomic statistical data. On this basis, we integrated existing pollen records from both regions and conducted a comparative analysis to examine evolutionary trajectories, driving mechanisms, and regional heterogeneity in China's terrestrial ecosystems. The study aims to address the following scientific questions: (1) How have the vegetation–climate–human activity relationships changed in typical lakes of northern China over the past two centuries? (2) How have vegetation successions in the monsoon and arid regions of China responded to climate change and socioeconomic development, and do the response processes and magnitudes exhibit regional differences?

2. Study area

Lake Gonghai ($38^{\circ}54'N$, $112^{\circ}14'E$; 1860 m a.s.l.), situated in Ningwu County, Shanxi Province, is an alpine enclosed lake with a surface area of 0.36 km^2 . The site lies within the monsoon region of northern China and is characterized by a temperate continental climate, with a mean annual temperature of 6.8°C and mean annual precipitation of 468 mm. Vegetation in the area is dominated by warm-temperate deciduous broad-leaved forests (Fig. 1d), primarily composed of *Betula platyphylla* and *Quercus liaotungensis*, with coniferous stands of *Picea wilsonii* and *Pinus tabuliformis*. Shrub and herb communities include *Kobresia myosuroides*, *Rosa davurica*, *Ostryopsis davidiana*, and *Hippophae rhamnoides* (Xu et al., 2017). Ningwu County has a permanent population of 133,700 and achieved a gross domestic product (GDP) of CNY 11.508 billion in 2023 (Ningwu County People's Government, 2023). The regional economy is primarily based on coal-dominated mining, agropastoral activities, and natural resource-based industries.

Lake Yueliang ($38^{\circ}27'N$, $105^{\circ}9'E$; 1295 m a.s.l.), situated in Alxa Left Banner, Alxa League, Inner Mongolia, is a desert-enclosed lake with a surface area of 4.2 km^2 . Located within the arid region of northern China, the area is characterized by a temperate continental climate, with a mean annual temperature of 9.1°C and mean annual precipitation of 208 mm. Located in the hinterland of the Tengger Desert, the regional vegetation is dominated by xerophytic shrub and semi-shrub communities (Fig. 1c), including members of the families Asteraceae, Poaceae, Polygonaceae, Zygophyllaceae, and *Tamarix*. Lakeside vegetation primarily consists of *Hedysarum scoparium* Fisch. & C.A.Mey., *Calligonum mongolicum* Turcz., and *Haloxylon ammodendron* Bunge (Duan et al., 2024). Alxa Left Banner has a permanent population of 203,000 and achieved a gross domestic product (GDP) of CNY 33.393 billion in 2023 (Alxa Left Banner People's Government, 2025). The regional economy is

Table 1

Geographical information of terrestrial pollen records from the monsoon and arid regions over the past two centuries.

ID	Name	Longitude (°)	Latitude (°)	Type	Time Period (CE)	Region	References
1	Lake Five-linked-great-pool	126.42	48.99	Lake	1836–2009	Monsoon region	Li J., 2015
2	Lake Keqin ^a	124.18	47.18	Lake	1825–2005	Monsoon region	Mackenzie et al., 2018
3	Lake Lianhuan	124.12	46.56	Lake	1790–2010	Monsoon region	Wang et al., 2022
4	Lake Hongyan	123.23	47.21	Lake	1890–1995	Monsoon region	Mackenzie et al., 2018
5	Lake Longjiang	123.08	46.51	Lake	1820–2009	Monsoon region	Mackenzie et al., 2018
6	Peatland Tuqiang	122.85	52.94	Peatland	1860–2016	Monsoon region	Han et al., 2021
7	Lake AerTianchi	120.40	47.32	Lake	1524–2010	Monsoon region	Li X., 2015
8	Lake Changdang ^a	119.53	31.62	Lake	1905–2016	Monsoon region	Ge et al., 2019
9	Lake Dalinur ^a	116.66	43.38	Lake	1597–2006	Arid region	Che, 2022
10	Lake Baiyangdian	116.03	38.82	Lake	1938–2018	Monsoon region	Ge et al., 2022
11	Lake Baiyangdian	116.00	38.84	Lake	1270–2009	Monsoon region	Fan et al., 2019
12	Lake Baiyangdian	115.98	38.94	Lake	1945–2018	Monsoon region	Ge et al., 2022
13	Lake Wanghu	115.55	29.86	Lake	1876–2006	Monsoon region	Yu, 2011
14	Lake Xiariburidu	114.93	42.72	Lake	1906–2006	Arid region	Zhang, 2015
15	Lake Liangzi ^a	114.62	30.17	Lake	1857–2008	Monsoon region	Ge et al., 2021
16	Reservoir Huangdong	114.57	22.95	Reservoir	1946–2010	Monsoon region	Chen et al., 2013
17	Lake Dailai	113.87	40.67	Lake	1393–1983	Arid region	Zhang, 2009
18	Lake Chiba Oxbow	113.00	29.58	Lake	1943–2012	Monsoon region	Jia et al., 2017
19	Lake Zhongzhouzi Oxbow	112.75	29.80	Lake	1940–2012	Monsoon region	Gao et al., 2016
20	Tian'e Zhou	112.57	29.85	Lake	1916–2012	Monsoon region	Jia et al., 2017
21	Lake Gonghai ^a	112.24	38.91	Lake	1842–2019	Monsoon region	This study
22	Lake Hongjiannao	110.24	39.11	Lake	1927–2000	Arid region	Xiao, 2005
23	Bay Yingluo	109.76	21.48	Bay	1810–2011	Monsoon region	Zhou, 2014
24	Bay Yingluo	109.76	21.49	Bay	1670–2011	Monsoon region	Zhou, 2014
25	Bay Yingluo	109.76	21.5	Bay	1810–2006	Monsoon region	Zhou, 2014
26	Mountain Zhongliang ^a	106.44	29.78	Karst depression	1274–2000	Monsoon region	Wang et al., 2021
27	Lake Yueliang ^a	105.15	38.46	Lake	1845–2020	Arid region	This study
28	Hongliujing	91.00	39.97	Tamarix cone	1832–2019	Arid region	Wang, 2024
29	Sichanghu ^a	89.2	44.1	Peatland	1561–2011	Arid region	Ren et al., 2020
30	Kongquehe ^a	87.88	40.96	Tamarix cone	1784–2019	Arid region	Wang, 2024
31	Andier ancient city	83.71	37.83	Tamarix cone	1792–2010	Arid region	Zhao et al., 2015
32	Damagou	81.08	37.09	Tamarix cone	1590–2010	Arid region	Guo et al., 2016

^a Pollen records used for comparative analysis in Fig. 7.

relatively undiversified, relying mainly on pastoralism and the extraction of mineral resources, particularly coal and rare earth elements.

3. Materials and methods

3.1. Sediment coring and chronology

In November 2019, we obtained a 52-cm long sediment core from the central basin of Lake Gonghai (GH-19a; 112°14'6.2" E, 38°54'36.35" N). In August 2020, we obtained a 63-cm long sediment core from the Lake Yueliang (YL-20a; 105°9'14.53" E, 38°27'46.92" N). Both cores were subsampled at 0.5 cm intervals under field conditions, subsequently transported to the laboratory, and stored in climate-controlled freezers (-4 °C) for subsequent analytical processing.

The age models for Lake Gonghai and Lake Yueliang were established based on the chronology reported by Ji et al. (2023). Lake Gonghai's sediment record spans the age range of 1842–2019 CE, with an average sedimentation rate of 0.294 cm yr⁻¹ and a temporal resolution of 3.4 years. The Lake Yueliang sequence covers 1845–2020 CE, with an average sedimentation rate of 0.360 cm yr⁻¹ and a temporal resolution of 2.7 years.

3.2. Pollen and fungal spore analysis

Pollen extraction was conducted using the standard HCl-NaOH-HF protocol (Faegri et al., 1989). Approximately 1 g samples were processed for pollen analysis. One tablet of *Lycopodium* spores (10,315 ± 350 grains/tablet) was added to each sample as a tracer for calculating the pollen concentration. All pollen and spores were identified under ×400 magnification using an Olympus DP-74 microscope to a sum of over 400 grains. Fungal spore analysis was executed concurrently with pollen counting, with fungal spore enumeration conducted only when pollen counts exceeded 400 grains. All pretreatment and analytical

procedures were completed at the Key Laboratory of Western China's Environmental Systems (Ministry of Education), Lanzhou University. Pollen and fungal spore percentage diagrams, along with concentration profiles, were generated using *Tilia* software (Grimm, 2004), with stratigraphic zones delineated through constrained incremental sum of squares (CONISS) cluster analysis.

4. Results

4.1. Lake Gonghai pollen and fungal spore results

The 52 samples analyzed from core GH-19a contained 25,663 pollen and spore grains, with an average of 494 grains per sample. The assemblage comprises 57 taxa, including 18 tree taxa, 7 shrub taxa, 28 herb taxa, and 4 fern spore types. The pollen percentage diagram shows trees accounted for 9.2 %, shrubs for 5.7 %, herbs for 84.9 %, and ferns for 0.2 % of the pollen sum. In addition, the pollen concentration diagram is provided in Supplementary Fig. 1. CONISS was used to conduct stratigraphically constrained cluster analysis on the pollen percentage data, which resulted in the definition of three pollen assemblage zones (Fig. 2).

Zone 1 (51–35 cm; 1843–1900 CE). The total pollen concentration was the lowest in the study sequence, with an average of 19,031 grains/g. Herb pollen dominated the assemblage (average of 87.2 %), primarily comprising *Artemisia* (average of 66.5 %), Amaranthaceae (average of 10.5 %), and Poaceae (average of 3.2 %), with trace occurrences of *Stellera*. Tree pollen accounted for 9.2 % of the total sum, dominated by *Betula*, followed by *Quercus*. Shrub pollen exhibited the lowest representation (average of 3.4 %), predominantly *Hippophae* and *Ostryopsis*.

Zone 2 (35–17 cm; 1900–1960 CE). The total pollen concentration showed an increase compared to the preceding zone (average of 20,662 grains/g). Herb pollen attained the highest percentage within the study sequence (average of 90.2 %), with *Artemisia* peaking at an average of

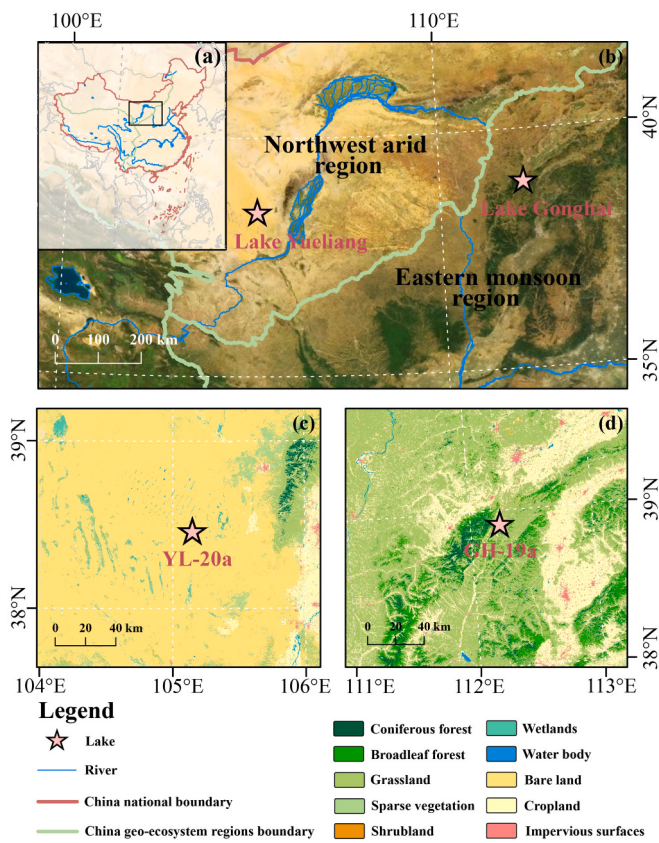


Fig. 1. Geographical setting of Lakes Gonghai (GH) and Yueliang (YL). (a) Location of the study area in Asia (the red line denotes China's national boundary). (b) Locations of Lakes Gonghai and Yueliang (pink asterisks) in relation to major rivers and topographic features (blue lines indicate major rivers; green lines represent boundaries of China's geo-ecosystem regions). (c) Vegetation map of the area surrounding Lake Yueliang (YL-20a). (d) Vegetation map of the area surrounding Lake Gonghai (GH-19a). (For interpretation of the references to colour in this figure legend, the reader is referred to the web version of this article.)

69.8 %, while Amaranthaceae declined to an average of 9.4 %, and *Stellera* exhibited a marginal decrease. Tree pollen demonstrated a marked reduction to an average of 5.6 %. Shrub pollen increased to an average of 4 %.

Zone 3 (17–0 cm; 1960–2019 CE). The total pollen concentration reached the highest level in the study sequence (average of 44,887 grains/g). Herb pollen decreased sharply to an average of 76.4 %, with marked declines in *Artemisia* (average of 58 %) and Amaranthaceae (average of 6.1 %), while *Stellera* exhibited a pronounced reduction compared to the previous two pollen zones. Tree pollen increased significantly to an average of 13.1 %, primarily driven by elevated proportions of *Pinus*, *Betula*, and *Quercus*. Shrub pollen attained the highest recorded value (average of 10.2 %), dominated by *Hippophae*.

The GH-19a core sequence yielded 27 fungal spore taxa, including 13 coprophilous types. In addition, the fungal spore concentration diagram is provided in Supplementary Fig. 2. CONISS cluster analysis divided the sequence into two primary zones, with Zone 2 further subdivided into two subzones (Fig. 3).

Zone 1 (51–23 cm; 1843–1940 CE). Characterized by peak coprophilous spores, dominated by *Sporormiella*-type (average of 27.6 %), *Sordaria* spp. (average of 5 %), and *Coniochaeta cf. lignaria* (average of 4.2 %), with other dung-related fungal spores <2 %. Other fungal spores featured *Glomus* sp. (average of 39.3 %), *Meliola* spp. (average of 4.6 %), and *Pleospora* spp. (average of 2.2 %), with remaining taxa <1.7 %.

Zone 2 (23–0 cm; 1940–2019 CE). Coprophilous spores decreased markedly, while other fungal spores increased. Subzone 2a (23–8 cm; 1940–1990 CE). The decline in *Sporormiella*-type (average of 12.5 %), *Sordaria* spp. (average of 4 %), and *Coniochaeta cf. lignaria* (average of 5.6 %), contrasting with elevated *Glomus* sp. (average of 50 %), *Meliola* spp. (average of 5.9 %), and *Pleospora* spp. (average of 4.4 %). Subzone 2b (8–0 cm; 1990–2019 CE). Slight rebound in coprophilous spores, dominated by *Sporormiella*-type (average of 16.1 %), *Sordaria* spp. (average of 8.0 %), and *Coniochaeta cf. lignaria* (average of 7.3 %), alongside decreased *Glomus* sp. (average of 40.3 %) and *Pleospora* spp. (average of 2.7 %), with *Meliola* spp. increasing to an average of 7.5 %.

4.2. Lake Yueliang pollen results

The 64 samples analyzed from core YL-20a contained 28,352 pollen and spore grains, with an average of 443 grains per sample. The assemblage comprises 56 taxa, including 20 tree taxa, 10 shrub taxa, 23 herb taxa, and 3 fern spore types. The pollen percentage diagram shows

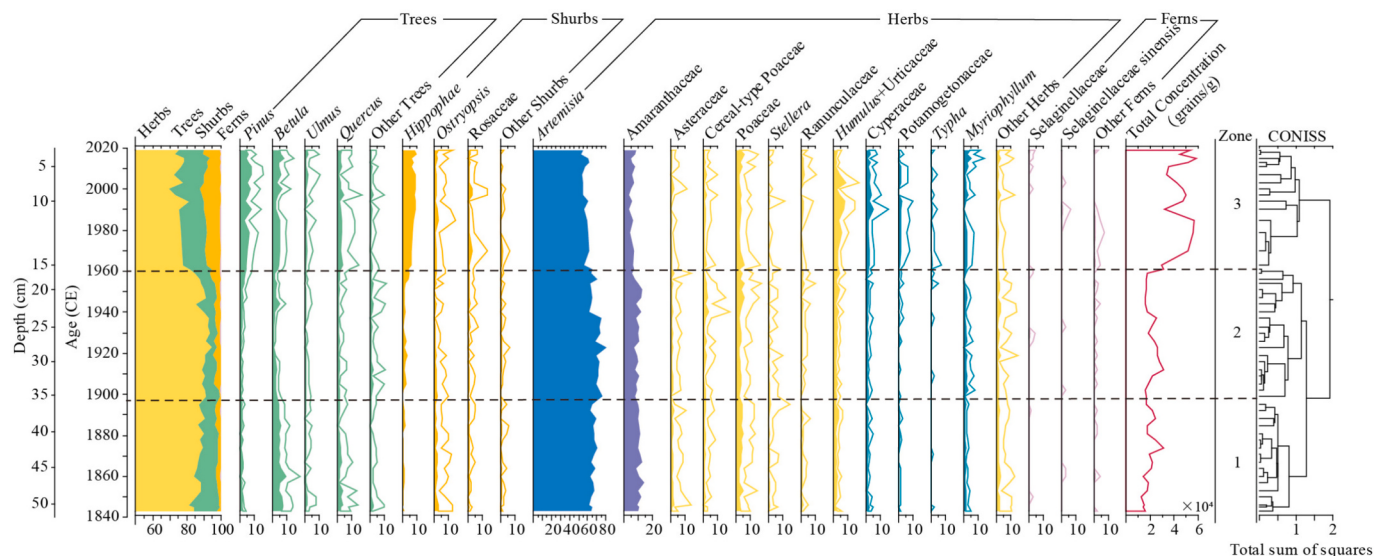


Fig. 2. Pollen percentage diagram of the GH-19a core (selected taxa shown only).

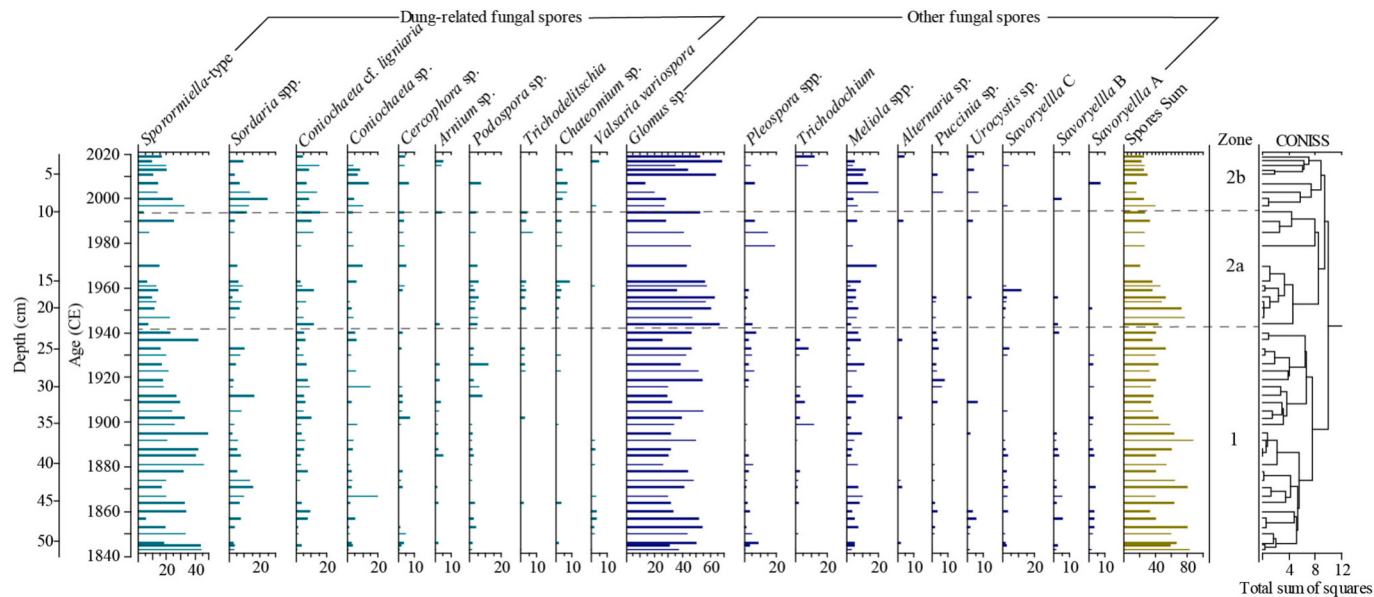


Fig. 3. Fungal spore percentage diagram of the GH-19a core (selected taxa shown only).

trees accounted for 2.8 %, shrubs for 4.7 %, herbs for 92.4 %, and ferns for 0.1 % of the pollen sum. In addition, the pollen concentration diagram is provided in Supplementary Fig. 3. CONISS cluster analysis divided the sequence into three pollen zones, with Zone 3 further subdivided into three subzones (Fig. 4).

Zone 1 (63–56 cm; 1846–1870 CE). The total pollen concentration (average of 59,151 grains/g) was the highest in the study sequence but showed a gradual decline. Herb pollen dominated the assemblage (average of 94.2 %), primarily comprising *Artemisia* (average of 59.5 %), Amaranthaceae (average of 15.2 %), and Poaceae (average of 17.2 %), with hygrophilous herbs being rare. Tree pollen remained low (average of 1.4 %), and shrub pollen (average of 4.3 %) was dominated by *Tamarix* (average of 3.1 %).

Zone 2 (56–43 cm; 1870–1904 CE). The total pollen concentration decreased markedly (average of 40,111 grains/g). Herb pollen (average of 93.1 %) exhibited increased *Artemisia* (average of 65 %) and Amaranthaceae (average of 20 %), while Poaceae declined sharply (average of 5.5 %). Hygrophilous herbs showed no significant changes. Tree (average of 1.8 %) and shrub pollen (average of 5 %) increased slightly, with *Tamarix* (average of 3.3 %) reaching its highest abundance in the

study sequence and *Nitraria* (average of 0.8 %) showing a minor rise.

Zone 3 (43–0 cm; 1904–2019 CE). Herb pollen was dominated by *Artemisia*, Amaranthaceae, and Poaceae, while hygrophilous herbs included Cyperaceae and Potamogetonaceae. Tree pollen increased, primarily comprising *Pinus*, *Quercus*, and *Betula*, while shrub pollen shifted to *Nitraria* and *Tamarix*. Subzone 3a (43–35 cm; 1904–1930 CE). Total pollen concentration plummeted (average of 18,887 grains/g). *Artemisia* (average of 59.8 %) and Amaranthaceae (average of 18.9 %) decreased slightly, while Poaceae (average of 11.4 %) and Cyperaceae (average of 1.8 %) rose. Tree pollen increased marginally (average of 2.5 %), and shrub dominance transitioned from *Tamarix* (average of 0.4 %) to *Nitraria* (average of 2.3 %). Subzone 3b (35–12 cm; 1930–1990 CE). Pollen concentration recovered slightly. *Artemisia*, Amaranthaceae, and Cyperaceae increased, while Poaceae declined (average of 6.4 %). Tree pollen remained stable, with *Nitraria* (average of 3 %) and *Tamarix* (average of 1.2 %) showing minor increases. Subzone 3c (12–0 cm; 1990–2019 CE). Pollen concentration rose moderately. Herb and shrub compositions remained stable, while tree pollen increased significantly (average of 6.2 %).

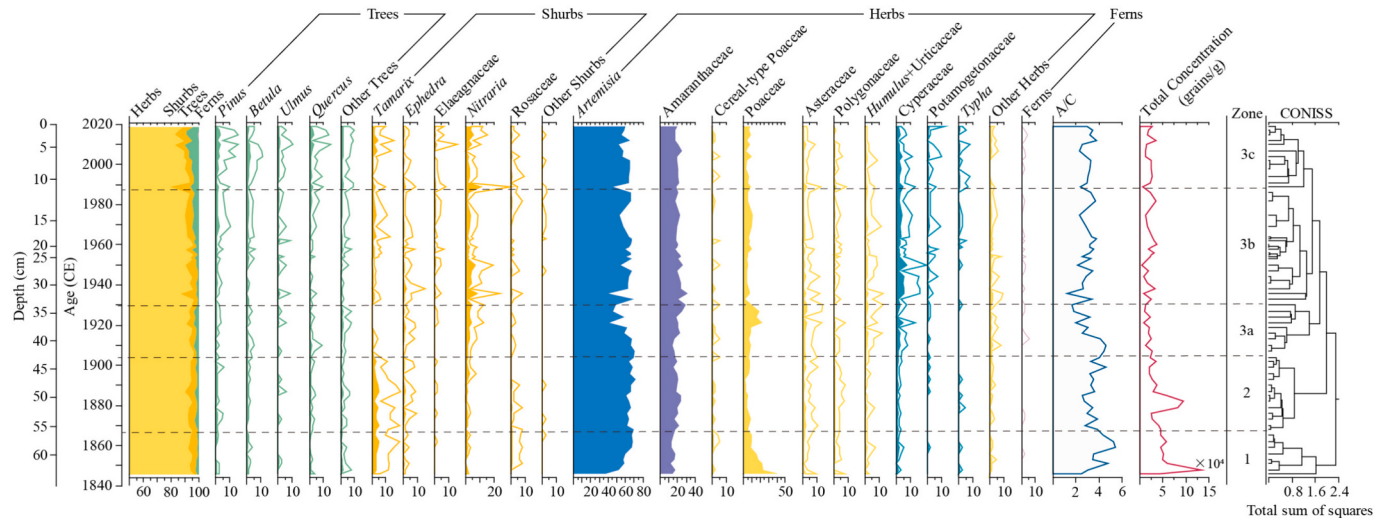


Fig. 4. Pollen percentage diagram of the YL-20a core (selected taxa shown only).

5. Discussion

5.1. Vegetation succession in Lake Gonghai of the monsoon region of China over the past two centuries

The vegetation succession history of the Lake Gonghai region over the past two centuries is divided into three distinct phases for analysis.

Prior to 1900 CE, arboreal vegetation abundance reached its highest levels (Fig. 5e), with *Betula* as the dominant genus, reflecting a humid climate favorable to forest development (Shen et al., 2008). However, the subsequent decline in arboreal vegetation may be attributed to deforestation caused by land reclamation practices during the Qing Dynasty (Ma et al., 1997). *Sporormiella*-type fungal spores, which derive primarily from herbivore dung and are closely associated with the activity of large grassland herbivores (Huang X et al., 2021; Raper and Bush, 2009; Wei et al., 2021; Zhang et al., 2021), peaked during this phase (Fig. 5d), indicating substantial grazing herbivore populations and intensive pastoral activities around Lake Gonghai. A concurrent increase in *Stellera* (*Stellera chamaejasme*) pollen, a recognized indicator of grassland degradation and overgrazing (Huang et al., 2017), alongside high coprophilous spore values, collectively signal grassland deterioration driven by intensified pastoralism. Historical records indicate that Ningwu County has long been a transitional zone between nomadic and agricultural cultures, with the study area in the northern part of the county historically centered on pastoral production, which supports the evidence of intensive pastoral activities (Ningwu County People's Government, 2023). During this phase, vegetation dynamics were jointly influenced by climate and human activities, with a relatively low population (Fig. 5b), and extensive pastoral activities coexisted with

relatively intact natural vegetation.

During 1900–1960 CE, arboreal vegetation declined to its lowest levels (Fig. 5e), potentially influenced by cold and dry climatic conditions (Cai et al., 2010; Shen et al., 2008). Historical records also document a simultaneous decline in forest cover across Shanxi Province (He et al., 2007), consistent with the observed arboreal vegetation decline. Meanwhile, a decrease in *Sporormiella*-type fungal spores suggests a reduction in herbivore populations and pastoral activity, which may have enabled partial grassland recovery (Dong et al., 2020). However, persistent occurrences of *Stellera* pollen indicate sustained grassland degradation despite reduced grazing intensity. Additionally, during the late Qing Dynasty and early Republican period, social instability and frequent wars led to widespread destruction and depletion of forest resources. Moreover, natural disasters such as floods and droughts severely impacted agricultural and pastoral production (Editorial Committee of Ningwu County Annals, 2001). Jiang et al. (2023) analyzed the variations in geochemical elements such as Al and Ca in Lake Gonghai sediments as indicators of human impact on surface weathering intensity. Their findings indicate that Al and Ca concentrations decreased during 1900–1950 CE, suggesting reduced agricultural activity associated with wartime disruptions. Consequently, climatic aridification and social instability during this phase synergistically drove vegetation degradation and hindered agro-pastoral development, culminating in regional environmental deterioration.

After 1960 CE, arboreal vegetation has increased markedly, particularly *Pinus* and *Betula*. Unlike the long-term trend since the mid-Holocene, when arboreal vegetation generally declined with decreasing precipitation (Chen et al., 2015; Xu et al., 2017), arboreal vegetation since 1960 CE has risen notably despite regional records

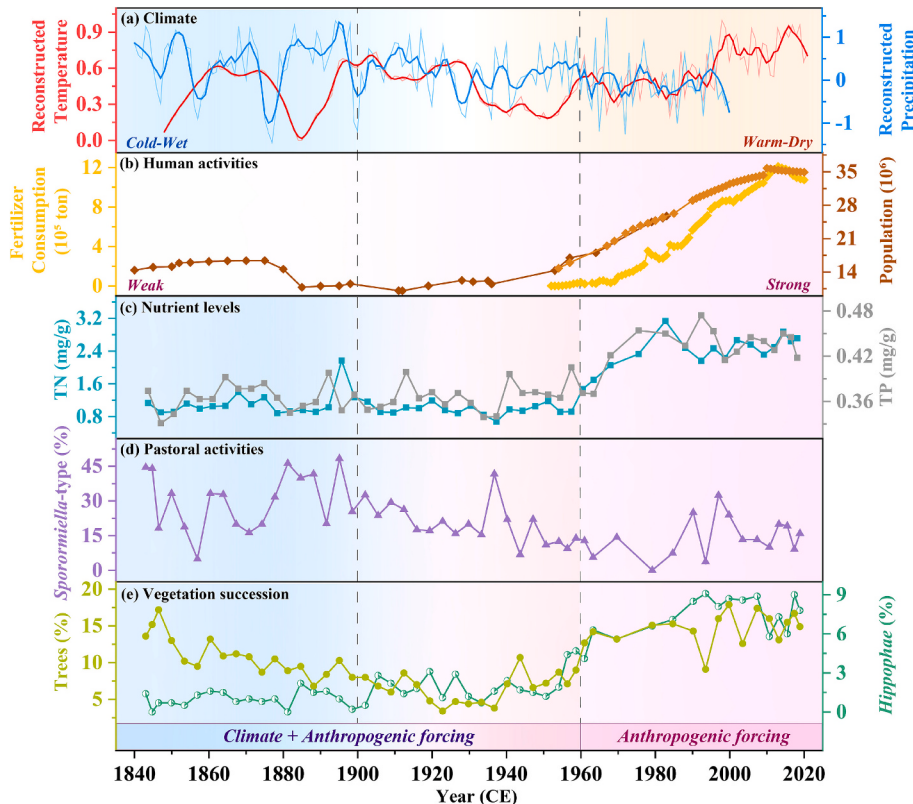


Fig. 5. Comparison of terrestrial pollen indicators from the GH-19a core with climate and anthropogenic records. (a) Tree-ring-based temperature reconstruction from Bei Wudang Mountain (Cai et al., 2010) and precipitation reconstruction (dry-wet index) for northern China (Shen et al., 2008). The transition from light blue to light orange indicates a climatic shift from cold-wet to warm-dry conditions. (b) Chemical fertilizer application and total population data in Shanxi Province (Shanxi Provincial Bureau of Statistics, 2023; Zhao and Xie, 1988). The gradual darkening of the pink shading reflects increasing intensity of human activities. (c) Sedimentary total nitrogen (TN) and total phosphorus (TP) concentrations (Ji et al., 2023). (d) Percentage of coprophilous fungal spores (*Sporormiella*-type). (e) Pollen percentages of trees and *Hippophae*. (For interpretation of the references to colour in this figure legend, the reader is referred to the web version of this article.)

indicating increasingly arid conditions (Shen et al., 2008). This change represents a clear departure from past natural variability (Supplementary Fig. 4). Moreover, given its temporal coincidence with large-scale afforestation initiatives (Shanxi Provincial Local History Compilation Committee Office, 1988), this expansion was most likely driven by anthropogenic activities. Concurrently, pollen concentration peaked during this phase (Fig. 2), while *Stellera* declined significantly, collectively indicating enhanced vegetation biomass and effective ecological restoration through active human management in the lacustrine periphery. In the early years of the People's Republic of China, north-western Shanxi faced severe land desertification (Ma and Su, 1996). To address this crisis, a series of ecological restoration programs including grazing prohibition, mountain closure for forest regeneration, and afforestation campaigns were systematically implemented (Shanxi Provincial Local History Compilation Committee Office, 1988). The provincial forest cover increased dramatically from 2.4 % in 1949 CE to 13.8 % by 1985 CE, following intensive afforestation efforts initiated in 1960 CE (Shanxi Provincial Local History Compilation Committee Office, 1988). The decline of *Sporormiella*-type fungal spores to their lowest levels reflects diminished pastoral activities, whereas *Hippophae* peaked (Fig. 5e), suggesting that artificial *Hippophae* planting, as a key agricultural activity, replaced some pastoral practices and became a significant economic source for the region (Yao and Zhu, 1985). The decline of pastoralism in northern China was influenced not only by grazing prohibition policies but also by the reduction in feed and grassland resources due to population growth and ecological changes (Wang, 2009). These factors collectively contributed to the transformation of the region's agricultural and pastoral systems. During this phase, the regional population grew rapidly, and with the implementation of ecological restoration policies, both vegetation and the

overall ecological environment significantly improved, while pastoral activities diminished and gradually transitioned to agriculture focused on *Hippophae* cultivation. However, intensified human activities have also contributed to lake eutrophication (Ji et al., 2023). Notably, the terrestrial (Fig. 5e) and lacustrine (Fig. 5c) ecosystems exhibited consistent trajectories of change.

5.2. Vegetation succession in Lake Yueliang of the arid region of China over the past two centuries

The vegetation succession history of the Lake Yueliang region over the past two centuries is divided into three distinct phases for analysis.

Prior to 1910 CE, the vegetation in the study area was dominated by terrestrial herb taxa such as *Artemisia* and Poaceae, with Poaceae reaching its peak abundance, accompanied by shrub taxa such as *Tamarix*. Both the *Artemisia*/Chenopodiaceae (A/C) ratio and pollen concentration peaked during this phase (Figs. 6d and 4), reflecting relatively humid regional conditions (Cai and Liu, 2007) that favored moisture-preferring *Artemisia* proliferation and high vegetation biomass around the lake. Consequently, this phase featured an *Artemisia*–*Tamarix* desert–steppe vegetation community. During 1910–1990 CE, a marked vegetation transition occurred, characterized by increased xerophytic Amaranthaceae, reduced Poaceae, and a shift in shrub dominance from *Tamarix* to *Nitraria* (Fig. 6d). The marked decline in pollen concentration indicates sparser surface vegetation cover, likely associated with increased evaporation due to regional temperature rise (Chen et al., 2016). Additionally, the expansion of Cyperaceae, which typically thrive in shallow waters or lakeside wetlands, may indicate that elevated temperatures caused lake-level decline, creating newly exposed habitats favorable for their growth. This phase marked a climate-driven

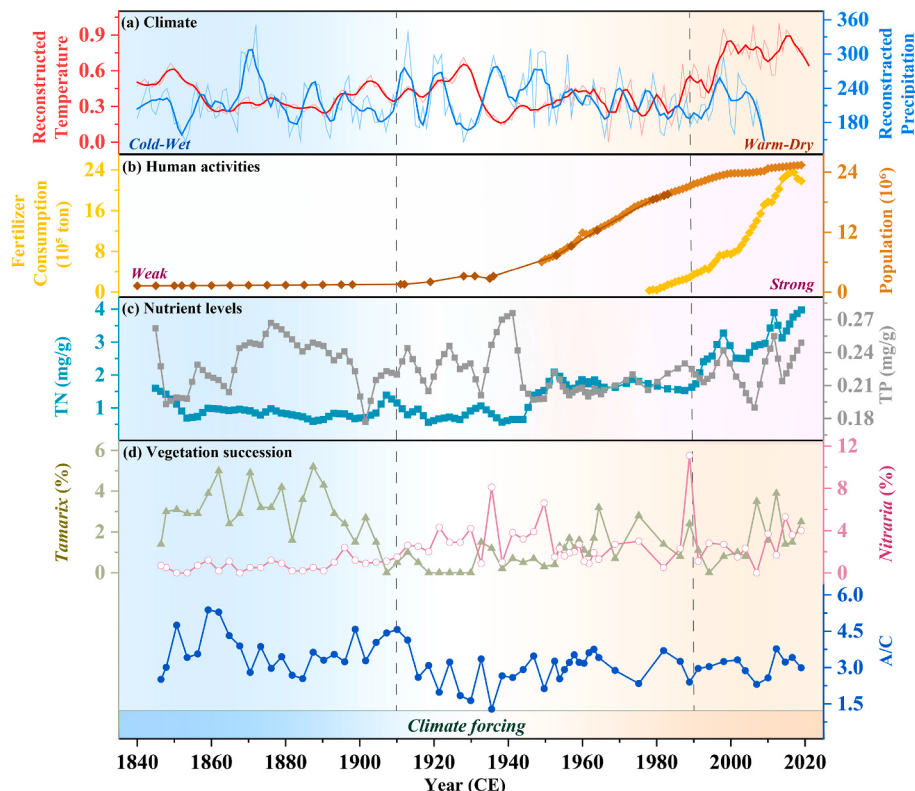


Fig. 6. Comparison of terrestrial pollen indicators from the YL-20a core with climate and anthropogenic records. (a) Tree-ring-based temperature and precipitation reconstructions from Helan Mountains (Cai and Liu, 2007; Chen et al., 2016). The transition from light blue to light orange indicates a climatic shift from cold-wet to warm-dry conditions. (b) Chemical fertilizer application and total population in Inner Mongolia (Inner Mongolia Autonomous Region Bureau of Statistics, 2023; Zhao and Xie, 1988). The gradual darkening of the pink shading reflects increasing intensity of human activities. (c) Sedimentary TN and TP concentrations (Ji et al., 2023). (d) Pollen percentages of *Tamarix* and *Nitraria*, alongside the pollen A/C ratio. (For interpretation of the references to colour in this figure legend, the reader is referred to the web version of this article.)

transition from *Artemisia-Tamarix* desert-steppe to *Amaranthaceae-Nitraria* desert-steppe vegetation. After 1990 CE, under a continued dry climate (Cai and Liu, 2007), vegetation has maintained a drought-resistant *Amaranthaceae-Nitraria* desert-steppe community with no further successional changes observed. The continued low values of the A/C ratio and pollen concentration, along with persistent Cyperaceae presence, reflect the ongoing impact of warm and arid conditions (Cai and Liu, 2007; Chen et al., 2016). This has led to a simplified vegetation structure with lower biomass, and the lake continues to shrink. Thus, the vegetation during this phase remains characterized by an *Amaranthaceae-Nitraria* desert-steppe community.

Notably, after 1990 CE, with the increase in regional population and the use of agricultural fertilizers (Fig. 6b), nitrogen emissions from agricultural production have led to increased atmospheric nitrogen deposition, resulting in a rapid rise in the total nitrogen (TN) content in lake sediments (Fig. 6c), thereby elevating the nutrient levels of the lake (Ji et al., 2023). Concurrently, the proliferation of submerged macrophytes such as *Potamogetonaceae* may be related to enhanced nutrient inputs (Fig. 4), creating favorable conditions for their growth (Huang F et al., 2021; Zhang et al., 2019). In contrast, terrestrial vegetation composition remained stable (Fig. 6d), while lacustrine ecosystems began responding to anthropogenic perturbations (Fig. 6e). This heightened sensitivity may stem from the fact that lakes, as closed or semi-closed aquatic systems, have lower biodiversity and weaker self-regulatory capacities compared to terrestrial ecosystems, making them more sensitive to environmental changes, particularly disturbances caused by human activities (Forzieri et al., 2022; Jeppesen et al., 2020; Zhou et al., 2024). Consequently, situated in a barren desert region with relatively limited human activities, Lake Yueliang has experienced limited anthropogenic impacts on its terrestrial vegetation. However, the lacustrine ecosystem, owing to its higher sensitivity, has exhibited earlier and more pronounced responses to external human disturbances.

5.3. Divergent trajectories and implications for terrestrial ecosystems in northern China

Northern China spans both the eastern monsoon region and northwestern arid region, which exhibit significant differences in climatic regimes, vegetation types, and socioeconomic activities. These differences have led to distinct ecosystem evolution patterns under the influence of climate change and human activities (Chen et al., 2025). This study, based on the classification of China's ecological geographic regions by Liu and Shi (2018), discusses the differences in the evolution of terrestrial ecosystems between the eastern monsoon region and the northwestern arid region (Fig. 7a).

The eastern monsoon region of China, predominantly influenced by the East Asian Summer Monsoon circulation, is characterized by a humid to semi-humid climate (Chen et al., 2019). The region supports diverse vegetation types and favorable ecological conditions, making it a densely populated and economically active area. Prior to 1900 CE, the region was transitioning from the late Little Ice Age to modern warming, and vegetation change was mainly driven by natural succession with limited human disturbance (Ge et al., 2010; Ge et al., 2021). After 1960 CE, however, rapid population growth has coincided with extensive industrial and agricultural production, resource extraction, and urbanization, profoundly altering the structure and functioning of natural ecosystems (Lin et al., 2024; Xie et al., 2021). This transformation has occurred broadly across the region (Fig. 7c). For instance, pollen records from several sites in northeastern China, including Lake Five-linked-great-pool (Li J, 2015), Lake Keqin (Mackenzie et al., 2018), and Peatland Tuqiang (Han et al., 2021), reveal that extensive deforestation and cropland reclamation led to a significant decline in natural forest taxa such as *Pinus*, accompanied by an increase in secondary forests dominated by *Betula*. With the continued advancement of agricultural intensification and urbanization, both cropland area and urban construction land have further expanded. For instance, pollen records from

several sites in northern and central China, including Lake Gonghai in North China, Lake Changdang (Ge et al., 2019), Lake Liangzi (Ge et al., 2021), and Lake Taibai (Xiao et al., 2013) in the middle and lower reaches of the Yangtze River, as well as the karst depression of Zhongliang Mountain (Wang et al., 2021), reveal a marked increase in cultivated crops such as Poaceae cereals and maize, along with anthropogenic indicator taxa such as *Hippophae* and *Juglans*, indicating a progressive transformation of the terrestrial ecosystem from forest-steppe landscapes to cropland-dominated vegetation. Additionally, highly intensive land use has contributed to natural wetland losses (Gao et al., 2016; Ge et al., 2022). Since the early years following the founding of the People's Republic of China, a nationwide afforestation policy known as the "universal forest protection" guideline was implemented (Zhou and Liang, 1950), resulting in increased tree cover and vegetation biomass in areas such as Lake Gonghai and Baiyangdian (Fan et al., 2019) in North China, indicating that vegetation in some areas was restored and improved during this phase. Subsequently, with the large-scale implementation of a series of ecological restoration policies, including the Grain-for-Green, shelterbelt development, and wetland restoration, vegetation has been significantly restored nationwide (Kong et al., 2022; Wang et al., 2022). Collectively, these findings suggest that over the past two centuries, vegetation succession in the eastern monsoon region of China has become increasingly dominated by human activities.

The northwestern arid region of China, predominantly influenced by the westerly circulation, is characterized by an arid to semi-arid climate (Chen et al., 2018; Chen et al., 2019). Sparse vegetation and fragile ecological conditions constrain economic development and population distribution in this region. Pollen records indicate that vegetation over the past two centuries has remained dominated by drought-tolerant herbs and xerophytic shrubs, with no fundamental shifts in community composition (Zhao et al., 2015). After 1960 CE, the region has shown a clear "warming and wetting" trend under global climate change (Chen et al., 2023; Ding et al., 2023). However, vegetation succession across different zones of the arid region exhibits marked regional differences, with response patterns showing a west-to-east transition from a warming-wetting trend to a warming-drying trend (Fig. 7b). For example, pollen records from the western zone of the arid region, such as the Kongquehe and Hongliujing in northern Lop Nur (Wang, 2024), the *Tamarix* cones in Damagou on the southern margin of the Taklimakan Desert (Guo et al., 2016), and the Peatland Sichanghu (Ren et al., 2020), indicate that after 1960 CE, there has been a decline in desert vegetation taxa such as *Tamarix* and *Ephedra*, along with an increase in the pollen A/C ratios. These changes reflect an increase in regional effective moisture under the influence of the westerlies (Huang et al., 2015; Wang et al., 2004). In contrast, the eastern zone of the arid region lies within the transitional belt of westerly-monsoon interactions, where climate variability is shaped by the interplay of westerly and monsoonal systems (Chen et al., 2021). Lake Yueliang, situated in this belt, is influenced by the summer monsoon and exhibits limited vegetation change, without a pronounced warming-wetting trend. Other areas closer to the monsoon boundary and more strongly influenced by summer monsoon circulation exhibit a warming-drying trend, consistent with the eastern monsoon region (Huang et al., 2015; Wang et al., 2004). For instance, pollen records from Lake Dalinur (Che, 2022) and Lake Xiariburidu in the eastern zone reveal that, after 1960 CE, vegetation coverage and pollen A/C ratios have both declined in response to this aridification trend. Furthermore, human activities have also contributed to local environmental changes. For instance, the appearance of crops along the southern edge of the Taklamakan Desert (Guo et al., 2016) and the demise of *Betula* forests in Lake Ebinur (Yan et al., 2021) and Wetland Habahe (Zhou Y et al., 2023) suggest that human activities may have contributed to localized environmental changes over the past two centuries. Collectively, these findings demonstrate that climate change remains the primary driver of vegetation succession in the northwestern arid region of China during the past two centuries, with limited

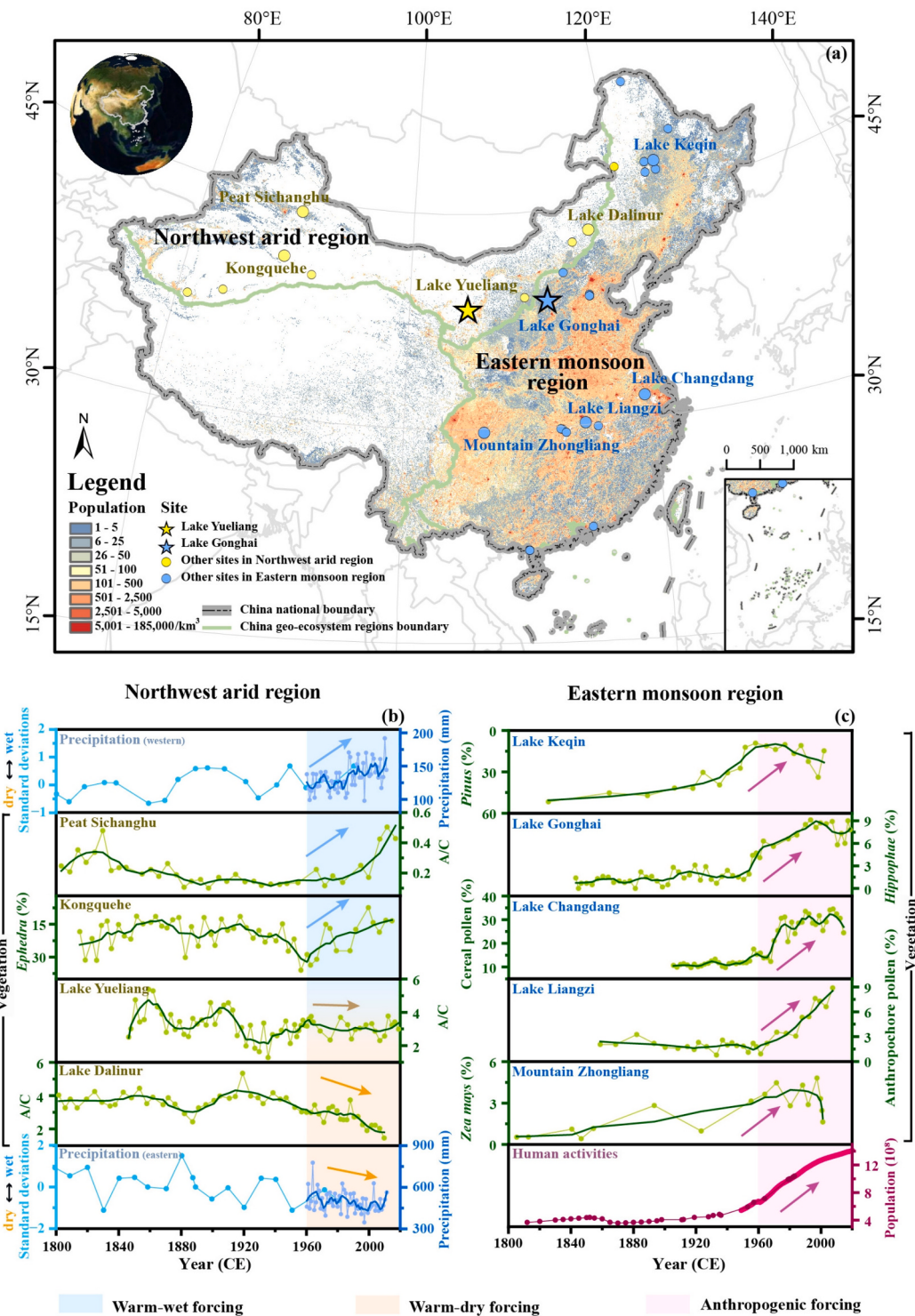


Fig. 7. Comparison of terrestrial pollen records between the monsoon and arid regions over the past two centuries. (a) Locations of pollen records and population density distribution (star symbols denote study sites Lake Gonghai and Lake Yueliang; circles represent additional compiled sites, Table 1). (b) Pollen and precipitation records from the arid region: regional paleo-precipitation series (Wang et al., 2004) and interannual precipitation variability (Huang et al., 2015) for the western arid zone, pollen A/C ratio from Peatland Sichanghu (Ren et al., 2020), pollen percentage of *Ephedra* from Kongquehe (Wang, 2024), pollen A/C ratio from Lake Yueliang, pollen A/C ratio from Lake Dalinur (Che, 2022), regional paleo-precipitation series (Wang et al., 2004) and interannual precipitation variability (Huang et al., 2015) for the eastern arid zone. Light blue shading denotes the warming-wetting phase; light orange shading denotes the warming-drying phase; blue-orange arrows indicate the west-east transition of vegetation responses in arid regions from warming-wetting to warming-drying. (c) Pollen and population records from the monsoon region: pollen percentage of *Pinus* from Lake Keqin (Mackenzie et al., 2018), pollen percentage of *Hippophae* from Lake Gonghai, percentage of cereal pollen from Lake Changdang (Ge et al., 2019), percentage of anthropochore pollen from Lake Liangzi (Ge et al., 2021), pollen percentage of *Zea mays* from Mountain Zhongliang karst depression (Wang et al., 2021), and total population for monsoon region (National Bureau of Statistics of China, 2023); light pink shading denotes the phase of intensified human activities; pink arrow represents the increasing dominance of human activities in driving vegetation changes in the monsoon region. (For interpretation of the references to colour in this figure legend, the reader is referred to the web version of this article.)

anthropogenic influence.

Unlike earlier climate-dominated patterns (Chen et al., 2015; Xu et al., 2017), the evolution of terrestrial ecosystems in northern China over the past two centuries has been increasingly shaped by the synergistic interplay between human activities and climate change, with more pronounced spatiotemporal heterogeneity compared to previous geological periods. After 1960 CE, pollen records from multiple sites in the eastern monsoon region have revealed a synchronous and significant increase in cultivated crops and anthropogenic indicator taxa (Ge et al., 2019, 2021; Wang et al., 2021), alongside a decrease in *Pinus* vegetation, coinciding with large-scale deforestation and land reclamation (Mackenzie et al., 2018). These vegetation changes, unaccompanied by significant climate shifts (Qin and Ding, 2022), suggest that anthropogenic forcing has become the dominant driver. In contrast, vegetation dynamics in the northwestern arid region follow a different pattern. In this region, the pollen A/C ratios and xerophyte proportions closely align with regional climate records (warming-wetting in western zone versus warming-drying in eastern zone) (Huang et al., 2015; Ren et al., 2020; Che, 2022; Wang, 2024). Meanwhile, the consistently low presence of crop pollen suggests weak human activity signals, further supporting the conclusion that vegetation succession in this region has been primarily climate-driven. Given these regional disparities, ecosystem restoration and conservation strategies should account for both climatic and anthropogenic influences and adopt region-specific management approaches. In the eastern monsoon region, where human impacts are pronounced, it is essential to strictly control the unregulated expansion of agricultural land and prioritize the restoration of natural vegetation through measures such as the Grain-for-Green Program and the construction of ecological corridors. In the climate-dominated northwest arid region, restoration efforts in the western subregion may leverage the warming and wetting trend, while in the eastern subregion, conservation of drought-tolerant vegetation and improved water resource management should be prioritized in response to the warming and drying trend.

6. Conclusions

To clarify vegetation-climate-human activity relationships in northern China, this study reconstructs vegetation succession over the past two centuries using high-resolution pollen records from Lake Gonghai (monsoonal region) and Lake Yueliang (arid region). The vegetation history of Lake Gonghai has been increasingly shaped by human activities and can be divided into three distinct stages. Prior to 1900 CE, vegetation dynamics were jointly influenced by humid climatic conditions and low-intensity human activities dominated by extensive pastoralism, with limited disturbance to natural vegetation. During 1900–1960 CE, climatic aridification and social instability led to vegetation degradation and a decline in pastoral activities, resulting in ecological deterioration. After 1960 CE, vegetation recovery has been observed, driven by ecological restoration policies, with a transition from traditional pastoralism to agriculture dominated by *Hippophae* cultivation. In contrast, vegetation succession at Lake Yueliang has been primarily driven by climate change, also progressing through three phases. Prior to 1910 CE, relatively humid conditions supported desert-steppe communities dominated by *Artemisia* and *Tamarix*. During 1910–1990 CE, increasing aridity led to a gradual transition toward desert-steppe vegetation dominated by Amaranthaceae and *Nitraria*. After 1990 CE, persistent aridity has maintained a stable desert-steppe community without significant compositional changes.

By synthesizing existing pollen records from both monsoonal and arid regions, this study reveals distinct spatial patterns in terrestrial ecosystem evolution across northern China over the past two centuries. In the eastern monsoon region, where the population is dense, vegetation dynamics have been primarily influenced by anthropogenic land-use transformations, with human activities becoming the primary driver after 1960 CE. In contrast, the northwestern arid region, with its

sparse population, vegetation is more sensitive to climate change. After 1960 CE, divergent climatic trends between the western (warming and wetting) and eastern (warming and drying) zones of the arid region have resulted in distinct vegetation successional responses. To achieve effective ecosystem restoration and promote balanced human-environment interactions, region-specific ecological restoration strategies should be implemented to address the dual pressures of global climate change and intensifying human activities.

CRediT authorship contribution statement

Jiaqi Pang: Writing – original draft, Formal analysis, Data curation. **Guoqiang Ding:** Writing – review & editing, Supervision, Investigation, Conceptualization. **Panpan Ji:** Investigation, Data curation. **Yuanhao Sun:** Supervision. **Chuanyi Duan:** Data curation. **Yu Cao:** Methodology. **Jiheng Shi:** Data curation. **Ruijin Chen:** Investigation. **Jianhui Chen:** Writing – review & editing, Supervision, Conceptualization.

Declaration of competing interest

The authors declare that they have no known competing financial interests or personal relationships that could have appeared to influence the work reported in this paper.

Acknowledgments

This work was supported by the Fundamental Research Funds for the Central Universities (Grant No. Izujbky-2025-it55), the National Natural Science Foundation of China (Grant No. 42401179), the China Postdoctoral Science Foundation (Grant No. 2024M761239), and the Postdoctoral Fellowship Program (Grade B) of China Postdoctoral Science Foundation (Grant No. GZB20240281). We thank Prof. Qinghai Xu, Prof. Yuecong Li, and Dr. Shengrui Zhang for their guidance on pollen identification, and Dr. Jun Zhang for assistance with fungal spore identification. We are also grateful to Dr. Xiuxiu Ren and Mr. Zezhou Zhu for their valuable suggestions during manuscript discussions.

Appendix A. Supplementary data

Supplementary data to this article can be found online at <https://doi.org/10.1016/j.palaeo.2025.113295>.

Data availability

The data used in this study can be obtained from <https://doi.org/10.6084/m9.figshare.29062331>.

References

- Alxa Left Banner People's Government, 2025. Regional Profile. Alxa Left Banner People's Government Website. Retrieved Month Day, Year, from. https://www.alsqz.gov.cn/art/2025/2/7/art_2156_6118.html (in Chinese).
- Batunacun Wieland, R., Lakes, T., Nendel, C., 2021. Using Shapley additive explanations to interpret extreme gradient boosting predictions of grassland degradation in Xilingol, China. Geosci. Model Dev. 14, 1493–1510. <https://doi.org/10.5194/gmd-14-1493-2021>.
- Berdugo, M., Gaitán, J.J., Delgado-Baquerizo, M., Crowther, T.W., Dakos, V., 2022. Prevalence and drivers of abrupt vegetation shifts in global drylands. Proc. Natl. Acad. Sci. 119, e2123393119. <https://doi.org/10.1073/pnas.2123393119>.
- Cai, Q.F., Liu, Y., 2007. January to August temperature variability since 1776 inferred from tree-ring width of *Pinus tabulaeformis* in Helan Mountain. J. Geogr. Sci. 17, 293–303. <https://doi.org/10.1007/s11442-007-0293-5>.
- Cai, Q.F., Liu, Y., Bao, G., Lei, Y., Sun, B., 2010. Tree-ring-based May–July mean temperature history for Lüliang Mountains, China, since 1836. Chin. Sci. Bull. 55, 3008–3014. <https://doi.org/10.1007/s11434-010-3235-z>.
- Cao, X.Y., Tian, F., Herzschuh, U., Ni, J., Xu, Q.H., Li, W.J., Zhang, Y.R., Luo, M.Y., Chen, F.H., 2022. Human activities have reduced plant diversity in eastern China over the last two millennia. Glob. Chang. Biol. 28, 4962–4976. <https://doi.org/10.1111/gcb.16274>.
- Chapin, F.S., Matson, P.A., Mooney, H.A., 2002. Principles of Terrestrial Ecosystem Ecology. Springer New York, New York, NY. <https://doi.org/10.1007/b97397>.

- Che, T.T., 2022. A 400-Year Vegetation and Climate History Inferred from Dali Lake Pollen Record, Inner Mongolia, China. China University of Geosciences, Beijing. [https://doi.org/10.27493/d.cnki.gzdzy.2016.000202 \(in Chinese\).](https://doi.org/10.27493/d.cnki.gzdzy.2016.000202)
- Chen, B.S., Zheng, Z., Huang, K.Y., Zheng, Y.W., Xu, Q.H., Zhang, Q.H., Huang, X.L., 2013. Sedimentation rate and environmental reconstruction based on grain-size and pollen-spores analysis from Huangdong Reservoir, Huizhou. *Geogr. Sci.* 33, 1259–1267. [https://doi.org/10.13249/j.cnki.sgs.2013.010.1259 \(in Chinese\).](https://doi.org/10.13249/j.cnki.sgs.2013.010.1259 (in Chinese).)
- Chen, F., Yuan, Y.J., Zhang, T.W., Linderholm, H.W., 2016. Annual precipitation variation for the southern edge of the Gobi Desert (China) inferred from tree rings: linkages to climatic warming of twentieth century. *Nat. Hazards* 81, 939–955. [https://doi.org/10.1007/s11069-015-2113-z.](https://doi.org/10.1007/s11069-015-2113-z)
- Chen, F.H., Chen, J.H., Huang, W., Chen, S.Q., Huang, X.Z., Jin, L.Y., Jia, J., Zhang, X.J., An, C.B., Zhang, J.W., Zhao, Y., Yu, Z.C., Zhang, R.H., Liu, J.B., Zhou, A.F., Feng, S., 2019. Westerlies Asia and monsoonal Asia: Spatiotemporal differences in climate change and possible mechanisms on decadal to sub-orbital timescales. *Earth Sci. Rev.* 192, 337–354. [https://doi.org/10.1016/j.earscirev.2019.03.005.](https://doi.org/10.1016/j.earscirev.2019.03.005)
- Chen, F.H., Huang, L.X., Cao, D.B., Chen, J., Chen, S.Q., Ma, S., Zhou, T.J., 2024. “Mega-sandwich pattern” of interdecadal precipitation variations and its regional manifestation in the Asian summer precipitation region. *Sci. Bull.* 69, 2656–2659. [https://doi.org/10.1016/j.scib.2024.06.026.](https://doi.org/10.1016/j.scib.2024.06.026)
- Chen, F.H., Xie, T.T., Yang, Y.J., Chen, S.Q., Chen, F., Huang, W., Chen, J., 2023. Discussion of the “warming and wetting” trend and its future variation in the drylands of Northwest China under global warming. *Sci. China Earth Sci.* 66, 1241–1257. [https://doi.org/10.1007/s11430-022-1098-x.](https://doi.org/10.1007/s11430-022-1098-x)
- Chen, F.H., Xu, Q.H., Chen, J.H., Birks, H.J.B., Liu, J.B., Zhang, S.R., Jin, L.Y., An, C.B., Telford, R.J., Cao, X.Y., Wang, Z.L., Zhang, X.J., Selvaraj, K., Lu, H.Y., Li, Y.C., Zheng, Z., Wang, H.P., Zhou, A.F., Dong, G.H., Zhang, J.W., Huang, X.Z., Bloemendal, J., Rao, Z.G., 2015. East asian summer monsoon precipitation variability since the last deglaciation. *Sci. Rep.* 5, 11186. [https://doi.org/10.1038/srep11186.](https://doi.org/10.1038/srep11186)
- Chen, J., Huang, W., Feng, S., Zhang, Q., Kuang, X.Y., Chen, J.H., Chen, F., 2021. The modulation of westerlies-monsoon interaction on climate over the monsoon boundary zone in East Asia. *Int. J. Climatol.* 41, E3049–E3064. [https://doi.org/10.1002/joc.6903.](https://doi.org/10.1002/joc.6903)
- Chen, J., Huang, W., Jin, L.Y., Chen, J.H., Chen, S.Q., Chen, F.H., 2018. A climatological northern boundary index for the East Asian summer monsoon and its interannual variability. *Sci. China Earth Sci.* 61, 13–22. [https://doi.org/10.1007/s11430-017-9122-x.](https://doi.org/10.1007/s11430-017-9122-x)
- Chen, S.Q., Sun, Y.H., Ding, G.Q., Cao, X.Y., 2025. Holocene dynamics of vegetation cover and their driving mechanisms in Asian drylands. *J. Earth Sci.* 36, 839–842. [https://doi.org/10.1007/s12583-025-0173-x.](https://doi.org/10.1007/s12583-025-0173-x)
- Ding, G.Q., Chen, J.H., Yan, H.Y., Zhang, S.R., Liu, Y., Zhou, A.F., Ji, P.P., Chen, S.Q., Lv, F.Y., Zhang, W.S., Ma, R., Chen, R.J., Chen, F.H., 2022. Late Holocene transition from natural to anthropogenic forcing of vegetation change in the semi-arid region of northern China. *Quat. Sci. Rev.* 287, 107561. [https://doi.org/10.1016/j.quascirev.2022.107561.](https://doi.org/10.1016/j.quascirev.2022.107561)
- Ding, Y.H., Liu, Y.J., Xu, Y., Wu, P., Xue, T., Wang, J., Shi, Y., Zhang, Y.X., Song, Y.F., Wang, P.L., 2023. Regional responses to global climate change: progress and prospects for trend, causes, and projection of climatic warming-wetting in Northwest China. *Adv. Earth Science* 38, 551–562. [https://doi.org/10.11867/j.issn.1001-8166.2023.027 \(in Chinese\).](https://doi.org/10.11867/j.issn.1001-8166.2023.027 (in Chinese).)
- Dong, S.K., Shang, Z.H., Gao, J.X., Boone, R.B., 2020. Enhancing sustainability of grassland ecosystems through ecological restoration and grazing management in an era of climate change on Qinghai-Tibetan Plateau. *Agric. Ecosyst. Environ.* 287, 106684. [https://doi.org/10.1016/j.agee.2019.106684.](https://doi.org/10.1016/j.agee.2019.106684)
- Duan, F.T., An, C.B., Wang, W., Zhao, Y.T., Zhou, A.F., 2024. A prolonged dry Mid-Holocene recorded by Moon Lake in the Tengger Desert, arid and semiarid China. *Quat. Res.* 117, 43–53. [https://doi.org/10.1017/qua.2023.77.](https://doi.org/10.1017/qua.2023.77)
- Editorial Committee of Ningwu County Annals, 2001. Ningwu County Annals. Red Flag Press, Beijing (in Chinese).
- Fægri, K., Kaland, P.E., Krzywinski, K., 1989. Textbook of pollen analysis. *J. Biogeogr.* 12, 328. [https://doi.org/10.2307/3038005.](https://doi.org/10.2307/3038005)
- Fan, B.S., Zhang, W.S., Zhang, R.C., Yang, X.L., Li, Y.C., Li, B., Ding, G.Q., 2019. Characteristics of dry-wet changes and human activities in the North China Plain since the Little Ice Age. *Quat. Sci.* 39, 483–496. [https://doi.org/10.11928/j.issn.1001-7410.2019.02.20 \(in Chinese\).](https://doi.org/10.11928/j.issn.1001-7410.2019.02.20 (in Chinese).)
- Forzieri, G., Dakos, V., McDowell, N.G., Ramdane, A., Cescatti, A., 2022. Emerging signals of declining forest resilience under climate change. *Nature* 608, 534–539. [https://doi.org/10.1038/s41586-022-04959-9.](https://doi.org/10.1038/s41586-022-04959-9)
- Fu, Y.S.H., Zhao, H.F., Piao, S.L., Peaucelle, M., Peng, S.S., Zhou, G.Y., Caias, P., Huang, M.T., Menzel, A., Peñuelas, J., Song, Y., Vitasse, Y., Zeng, Z.Z., Janssens, I.A., 2015. Declining global warming effects on the phenology of spring leaf unfolding. *Nature* 526, 104–107. [https://doi.org/10.1038/nature15402.](https://doi.org/10.1038/nature15402)
- Gao, X., Jia, T.F., Xu, Q.H., Wang, F., Wang, A., 2016. Records of lacustrine sedimentology and pollen-charcoal assemblages responding to climate change and human activities in Zhongzhouzi Oxbow Lake, Hubei Province for about 70 years. *Quat. Sci.* 36, 1445–1455. [https://doi.org/10.11928/j.issn.1001-7410.2016.06.10 \(in Chinese\).](https://doi.org/10.11928/j.issn.1001-7410.2016.06.10 (in Chinese).)
- García-Mozo, H., Oteros, J.A., Galán, C., 2016. Impact of land cover changes and climate on the main airborne pollen types in southern Spain. *Sci. Total Environ.* 548–549, 221–228. [https://doi.org/10.1016/j.scitotenv.2016.01.005.](https://doi.org/10.1016/j.scitotenv.2016.01.005)
- Ge, Q.S., Zheng, J.Y., Hao, Z.X., Shao, X.M., Wang, W.C., Luterbacher, J., 2010. Temperature variation through 2000 years in China: an uncertainty analysis of reconstruction and regional difference. *Geophys. Res. Lett.* 37, L03703. [https://doi.org/10.1029/2009GL041281.](https://doi.org/10.1029/2009GL041281)
- Ge, Y.W., Mao, X., She, Z.J., Liu, L.J., Song, L., Li, Y.C., Liu, C.H., 2022. Spatial heterogeneity of long-term environmental changes in a large agricultural wetland in North China: Implications for wetland restoration. *CATENA* 219, 106582. [https://doi.org/10.1016/j.catena.2022.106582.](https://doi.org/10.1016/j.catena.2022.106582)
- Ge, Y.W., Zhang, K., Yang, X.D., 2018. Long-term succession of aquatic plants reconstructed from palynological records in a shallow freshwater lake. *Sci. Total Environ.* 643, 312–323. [https://doi.org/10.1016/j.scitotenv.2018.06.203.](https://doi.org/10.1016/j.scitotenv.2018.06.203)
- Ge, Y.W., Zhang, K., Yang, X.D., 2019. A 110-year pollen record of land use and land cover changes in an anthropogenic watershed landscape, eastern China: Understanding past human-environment interactions. *Sci. Total Environ.* 650, 2906–2918. [https://doi.org/10.1016/j.scitotenv.2018.10.058.](https://doi.org/10.1016/j.scitotenv.2018.10.058)
- Ge, Y.W., Zhang, Q.H., Dong, X.H., Yang, X.D., 2021. Revealing anthropogenic effects on lakes and wetlands: Pollen-based environmental changes of Liangzi Lake, China over the last 150 years. *CATENA* 207, 105605. [https://doi.org/10.1016/j.catena.2021.105605.](https://doi.org/10.1016/j.catena.2021.105605)
- Grimm, E.C., 2004. *Tilia and TG View Version 2.0.2.* Illinois State Museum.
- Guo, F., Zhao, C., Zhao, Y.J., Xia, X.C., 2016. Pollen assemblages of *Tamarix* cone sedimentary veins and environmental change in the southern margin of taklimakan desert for about the last 400 years. *Acta Palaeontol. Sin.* 55, 136–144. [https://doi.org/10.19800/j.cnki.aps.2016.01.012 \(in Chinese\).](https://doi.org/10.19800/j.cnki.aps.2016.01.012 (in Chinese).)
- Han, D.X., Gao, C.Y., Liu, H.X., Li, Y.H., Cong, J.X., Yu, X.F., Wang, G.P., 2021. Anthropogenic and climatic-driven peatland degradation during the past 150 years in the Greater Khingan Mountains, NE China. *Land Degrad. Dev.* 32, 4845–4857. [https://doi.org/10.1002/ldr.4036.](https://doi.org/10.1002/ldr.4036)
- Hanke, W., Böhner, J., Dreber, N., Jürgens, N., Schmidel, U., Wesuls, D., Dengler, J., 2014. The impact of livestock grazing on plant diversity: an analysis across dryland ecosystems and scales in southern Africa. *Ecol. Appl.* 24, 1188–1203. [https://doi.org/10.1890/13-0377.1.](https://doi.org/10.1890/13-0377.1)
- He, F.N., Ge, Q.S., Dai, J.H., Lin, S.S., 2007. Quantitative analysis on forest dynamics of China in recent 300 years. *Acta Geograph. Sin.* 62, 30–40. [https://doi.org/10.11821/xb200701004 \(in Chinese\).](https://doi.org/10.11821/xb200701004 (in Chinese).)
- Huang, F.F., Zhang, K., Huang, S.X., Lin, Q., 2021a. Patterns and trajectories of macrophyte change in East China’s shallow lakes over the past one century. *Sci. China Earth Sci.* 64, 1735–1745. [https://doi.org/10.1007/s11430-020-9806-9.](https://doi.org/10.1007/s11430-020-9806-9)
- Huang, X.Y., Li, Y.H., Feng, J.Y., Wang, J.S., Wang, Z.L., Wang, S.J., Zhang, Y., 2015. Climate characteristics of precipitation and extreme drought events in Northwest China. *Acta Ecol. Sin.* 35, 1359–1370. [https://doi.org/10.5846/stxb201305101013 \(in Chinese\).](https://doi.org/10.5846/stxb201305101013 (in Chinese).)
- Huang, X.Z., Liu, S.S., Dong, G.H., Qiang, M.R., Bai, Z.J., Zhao, Y., Chen, F.H., 2017. Early human impacts on vegetation on the northeastern Qinghai-Tibetan Plateau during the middle to late Holocene. *Prog. Phys. Geogr.* 41, 286–301. [https://doi.org/10.1177/030913317703035.](https://doi.org/10.1177/030913317703035)
- Huang, X.Z., Zhang, J., Ren, L.L., Zhang, S.R., Chen, F.H., 2021b. Intensification and driving forces of pastoralism in Northern China 5.7 ka ago. *Geophys. Res. Lett.* 48, e2020GL092288. [https://doi.org/10.1029/2020GL092288.](https://doi.org/10.1029/2020GL092288)
- Inner Mongolia Autonomous Region Bureau of Statistics, 2023. Inner Mongolia Statistical Yearbook. China Statistics Press, Beijing (in Chinese).
- IPCC, 2021. Climate change 2021: The physical science basis. In: Contribution of Working Group I to the Sixth Assessment Report of the Intergovernmental Panel on Climate Change. Cambridge University Press.
- IPCC, 2023. Climate change 2023: Synthesis report. In: Contribution of Working Groups I, II and III to the Sixth Assessment Report of the Intergovernmental Panel on Climate Change [Core Writing Team, H. Lee & J. Romero (Eds.)]. IPCC.
- Jeppesen, E., Beklioğlu, M., Özkan, K., Akyürek, Z., 2020. Salinization increase due to climate change will have substantial negative effects on inland waters: a call for multifaceted research at the local and global scale. *Innovation* 1, 100030. [https://doi.org/10.1016/j.ximn.2020.100030.](https://doi.org/10.1016/j.ximn.2020.100030)
- Ji, P.P., Chen, J.H., Zhou, A.F., Chen, R.J., Ding, G.Q., Wang, H.P., Chen, S.Q., Chen, F.H., 2023. Anthropogenic atmospheric deposition caused the nutrient and toxic metal enrichment of the enclosed lakes in North China. *J. Hazard. Mater.* 448, 130972. [https://doi.org/10.1016/j.jhazmat.2023.130972.](https://doi.org/10.1016/j.jhazmat.2023.130972)
- Jia, T.F., Gao, X., Wang, F., 2017. Significance of pollen and charcoal characteristics to the oxbow environmental change events at Jingzhou the Yangtze River in recent 100 year: a case study of Tian’E and Chiba Lake. *Resour. Environ. Yangtze Basin* 26, 1630–1640. <https://doi.org/10.11870/cjlyzyyhj201710015> in Chinese.
- Jiang, H., Han, Y.M., Tang, Y.L., Fan, H.M., Liu, B., Arimoto, R., 2023. Elemental data for gonghai lake sediments show significant effects of human activities on weathering processes after 1550 CE. *Front. Earth Sci.* 10. [https://doi.org/10.3389/feart.2022.1043770.](https://doi.org/10.3389/feart.2022.1043770)
- Kong, X.S., Fu, M.X., Zhao, X., Wang, J., Jiang, P., 2022. Ecological effects of land-use change on two sides of the Hu Huanyong Line in China. *Land Use Policy* 113, 105895. [https://doi.org/10.1016/j.landusepol.2021.105895.](https://doi.org/10.1016/j.landusepol.2021.105895)
- Li, J., 2015. Pollen Characteristics and Environmental Significance of Five-Linked-Great-Pool Lake in Heilongjiang Province since the Last 200 Years. China University of Geosciences, Beijing (in Chinese).
- Li, X.L., 2015. Inner Mongolia the Aer Tianchi since the Little Ice Age lake drilling pollen characteristics and vegetation succession. China University of Geosciences, Beijing (in Chinese).
- Lin, Q., Zhang, K., Giguet-Covex, C., Arnaud, F., McGowan, S., Gielly, L., Capo, E., Huang, S.X., Ficetola, G.F., Shen, J., Dearing, J.A., Meadows, M.E., 2024. Transient social–ecological dynamics reveal signals of decoupling in a highly disturbed Anthropocene landscape. *Proc. Natl. Acad. Sci.* 121, e2321303121. [https://doi.org/10.1073/pnas.2321303121.](https://doi.org/10.1073/pnas.2321303121)
- Liu, C., Shi, R.X., 2018. GIS dataset of boundaries among four geo-eco regions of China. *J. Global Change Data Discov.* 2, 42–50. [https://doi.org/10.3974/geodp.2018.01.08.](https://doi.org/10.3974/geodp.2018.01.08)

- Lv, F.Y., Sun, Y.H., Wang, X.Q., Zhang, P.J., 2024. Precipitation changes and extreme drought events over the last millennium inferred from a pollen record from moon lake, Northeast China. *Palaeogeogr. Palaeoclimatol. Palaeoecol.* 640, 112089. <https://doi.org/10.1016/j.palaeo.2024.112089>.
- Ma, Y.J., Su, Z.Z., 1996. Research on the land desertification in the northwest of Shanxi Province. *J. Desert Res.* 16, 301–306 (in Chinese).
- Ma, Z.L., Song, C.S., Zhang, Q.H., 1997. The Changes of Forests in China. China Forestry Publishing House, Beijing (in Chinese).
- Mackenzie, L., Bao, K.S., Mao, L.M., Klamt, A.-M., Pratte, S., Shen, J., 2018. Anthropogenic and climate-driven environmental change in the Songnen Plain of northeastern China over the past 200 years. *Palaeogeogr. Palaeoclimatol. Palaeoecol.* 511, 208–217. <https://doi.org/10.1016/j.palaeo.2018.08.005>.
- McCulloch, M.T., Winter, A., Sherman, C.E., Trotter, J.A., 2024. 300 years of sclerosponge thermometry shows global warming has exceeded 1.5 °C. *Nat. Clim. Chang.* 14, 171–177. <https://doi.org/10.1038/s41558-023-01919-7>.
- National Bureau of Statistics of China, 2023. *China Population & Employment Statistical Yearbook*. China Statistics Press, Beijing (in Chinese).
- Ningwu County People's Government, 2023. Overview of Ningwu County in 2023. Ningwu County People's Government Website. Retrieved Month Day, Year, from. http://www.ningwu.gov.cn/zjnw/nwgl/202310/20231008_3914284.html (in Chinese).
- Piao, S.L., Huang, M., Liu, Z., Wang, X.H., Ciais, P., Canadell, J.G., Wang, K., Bastos, A., Friedlingstein, P., Houghton, R.A., Le Quéré, C., Liu, Y.W., Myreni, R.B., Peng, S.S., Pongratz, J., Sitch, S., Yan, T., Wang, Y.L., Zhu, Z.C., Wu, D.H., Wang, T., 2018. Lower land-use emissions responsible for increased net land carbon sink during the slow warming period. *Nat. Geosci.* 11, 739–743. <https://doi.org/10.1038/s41561-018-0204-7>.
- Poraj-Górska, A.I., Żarczyński, M.J., Ahrens, A., Enters, D., Weisbrodt, D., Tylmann, W., 2017. Impact of historical land use changes on lacustrine sedimentation recorded in varved sediments of Lake Jaczno, northeastern Poland. *CATENA* 153, 182–193. <https://doi.org/10.1016/j.catena.2017.02.007>.
- Qin, D.H., Ding, Y.J., 2022. *Climate and Ecological Environment Evolution in China*. Science Press, Beijing (in Chinese).
- Raper, D., Bush, M., 2009. A test of *sporormiella* representation as a predictor of megaherbivore presence and abundance. *Quat. Res.* 71, 490–496. <https://doi.org/10.1016/j.yqres.2009.01.010>.
- Ren, W.H., Zhao, Y., Li, Q., Chen, J.H., 2020. Changes in vegetation and moisture in the northern Tianshan of China over the past 450 years. *Front. Earth Sci.* 14, 479–491. <https://doi.org/10.1007/s11707-019-0788-2>.
- Rodríguez-Zorro, P.A., Enters, D., Hermanowski, B., Da Costa, M.L., Behling, H., 2015. Vegetation changes and human impact inferred from an oxbow lake in southwestern Amazonia, Brazil since the 19th century. *J. S. Am. Earth Sci.* 62, 186–194. <https://doi.org/10.1016/j.jsames.2015.06.003>.
- Shanxi Provincial Bureau of Statistics, 2023. *Shanxi Statistical Yearbook*. China Statistics Press, Beijing (in Chinese).
- Shanxi Provincial Local History Compilation Committee Office, 1988. *Shanxi Forestry Annals*. Shanxi People's Publishing House, Taiyuan (in Chinese).
- Shen, C.M., Wang, W.C., Hao, Z.X., Gong, W., 2008. Characteristics of anomalous precipitation events over eastern China during the past five centuries. *Clim. Dyn.* 31, 463–476. <https://doi.org/10.1007/s00382-007-0323-0>.
- Steffen, W., Broadgate, W., Deutscher, L., Gaffney, O., Ludwig, C., 2015. The trajectory of the anthropocene: the great acceleration. *Anthropocene Rev.* 2, 81–98. <https://doi.org/10.1177/2053019614564785>.
- Steegner, M.A., Spanbauer, T.L., 2023. North American pollen records provide evidence for macroscale ecological changes in the Anthropocene. *Proc. Natl. Acad. Sci. USA* 120, e2306815120. <https://doi.org/10.1073/pnas.2306815120>.
- Sun, Y.H., Zhang, S.R., Xu, Q.H., 2022. Pollen-based land cover changes reveal temporal and spatial differences of human activity in north-Central China during the Holocene. *Catena* 219, 106620. <https://doi.org/10.1016/j.catena.2022.106620>.
- Theuerkauf, M., Dräger, N., Kienel, U., Kuparinen, A., Brauer, A., 2015. Effects of changes in land management practices on pollen productivity of open vegetation during the last century derived from varved lake sediments. *Holocene* 25, 733–744. <https://doi.org/10.1177/0959683614567881>.
- Wang, C.F., Fu, X.D., Zhang, X.M., Wang, X.P., Zhang, G., Gong, Z., 2024a. Modeling soil erosion dynamic processes along hillslopes with vegetation impact across different land uses on the loess plateau of China. *CATENA* 243, 108202. <https://doi.org/10.1016/j.catena.2024.108202>.
- Wang, D.D., Xu, Q.H., Sun, Y.H., Zhang, S.R., 2025. Centennial to multidecadal scales variability of East Asian summer monsoon precipitation in North China during the Holocene. *Glob. Planet. Chang.* 245, 104692. <https://doi.org/10.1016/j.gloplacha.2025.104692>.
- Wang, J.G., 2009. *Ecology and Society in North China during the Late Traditional Period*. SDX Joint Publishing Company, Beijing (in Chinese).
- Wang, N., 2024. Response of *Tamarix* Cone Pollen Assemblage to Regional Environment in Northern Lop nor Region in Recent 200 Years. Hebei Normal University, Shijiazhuang (in Chinese).
- Wang, Q.R., Jiang, Y.J., Hao, X.D., Qiao, Y.N., Zhang, C.Y., Ma, L.N., Mao, Y., Lv, T.R., Qiu, J., 2021. A 700-year record of vegetation and rocky desertification evolution based on palynological data of the karst valley area, Chongqing City, China. *Acta Ecol. Sin.* 41, 3634–3644. <https://doi.org/10.5846/stxb202002080213> (in Chinese).
- Wang, T., Yang, B., Braeuning, A., Xia, D., 2004. Decadal-scale precipitation variations in arid and semiarid zones of northern China during the last 500 years. *Chin. Sci. Bull.* 49, 842–848. <https://doi.org/10.1007/BF02889758>.
- Wang, X.L., Xiao, H.F., Xiao, X.Y., 2022. Environmental changes and human activities over the last about 220 years revealed by the pollen record of Lake Lianhuan in Heilongjiang Province. *J. Lake Sci.* 34, 684–694. <https://doi.org/10.18307/2022.0227> (in Chinese).
- Wang, Y.X., Peng, L., Yue, Y.M., Chen, T.T., 2024b. Global vegetation-temperature sensitivity and its driving forces in the 21st century. *Earth's Future* 12, e2022EF003395. <https://doi.org/10.1029/2022EF003395>.
- Wei, H.C., Duan, R.L., Zhang, J., Sun, Y.J., Hou, G.L., Gao, J.Y., 2021. Fungal spore record of pastoralism on the NE Qinghai-Tibetan Plateau since the middle Holocene. *Sci. China Earth Sci.* 64, 1318–1331. <https://doi.org/10.1007/s11430-020-9787-4>.
- Xiao, X.Y., 2005. Sporopollen record and environmental evolution since ~ 100 years in Lake Hongjiannao, Shaanxi Province. *J. Lake Sci.* 17, 28–34. <https://doi.org/10.18307/2005.0105> (in Chinese).
- Xiao, X.Y., Yang, X.D., Shen, J., Wang, S.M., Xue, B., Tong, X.F., 2013. Vegetation history and dynamics in the middle reach of the Yangtze River during the last 1500 years revealed by sedimentary records from Taibai Lake, China. *Holocene* 23, 57–67. <https://doi.org/10.1177/0959683612450195>.
- Xie, Y., Wang, Y.B., Liu, X.Q., Shen, J., Wang, Y., 2021. Increasing human activities during the past 2,100 years in Southwest China inferred from a fossil pollen record. *Veg. Hist. Archaeobotany* 30, 477–488. <https://doi.org/10.1007/s00334-020-00799-7>.
- Xu, Q.H., Chen, F.H., Zhang, S.R., Cao, X.Y., Li, J.Y., Li, Y.C., Li, M.Y., Chen, J.H., Liu, J., B., Wang, Z.L., 2017. Vegetation succession and East Asian Summer Monsoon changes since the last deglaciation inferred from high-resolution pollen record in Gonghai Lake, Shanxi Province, China. *Holocene* 27, 835–846. <https://doi.org/10.1177/0959683616675941>.
- Xu, Q.H., Liu, H.Y., Zheng, Z., 2024. Challenges and opportunities in quaternary palynology. *Sci. China Earth Sci.* 67, 2148–2161. <https://doi.org/10.1007/s11430-023-1310-4>.
- Yan, Q.Y., Wang, L., Zhang, Y., Kong, Z.C., Chen, L.X., Yang, Z.J., 2021. Changes in vegetation and environment in the *Betula microphylla* wetland of Ebinur Lake in Xinjiang, China since 3900 cal. aBP. *J. Appl. Ecol.* 32, 486–494. <https://doi.org/10.13287/j.1001-9332.202102.007> (in Chinese).
- Yao, Y.M., Zhu, C.J., 1985. Investigation report on wild sea buckthorn resources in the western plateau region of Shanxi. *Shanxi Forest. Sci. Technol.* 32–35, 25 (in Chinese).
- Yu, G., 2011. High-resolution records of lacustrine sedimentology and palynology responding to changes in climate and hydrology. *Acta Sedimentol. Sin.* 29, 118–124. <https://doi.org/10.14027/j.cnki.cjxb.2011.01.008> (in Chinese).
- Yue, C., Xu, M.Y., Ciais, P., Tao, S., Shen, H.Z., Chang, J.F., Li, W., Deng, L., He, J.H., Leng, Y., Li, Y., Wang, J.M., Xu, C., Zhang, H., Zhang, P.Y., Zhang, L.K., Zhao, J., Zhu, L., Piao, S.L., 2024. Contributions of ecological restoration policies to China's land carbon balance. *Nat. Commun.* 15, 9708. <https://doi.org/10.1038/s41467-024-54100-9>.
- Zalasiewicz, J., Waters, C.N., Ellis, E.C., Head, M.J., Vidas, D., Steffen, W., Thomas, J.A., Horn, E., Summerhayes, C.P., Leinfelder, R., McNeill, J.R., Gatuszka, A., Williams, M., Barnosky, A.D., de Richter, D.B., Gibbard, P.L., Syvitski, J., Jeandel, C., Ceareta, A., Cundy, A.B., Fairchild, I.J., Rose, N.L., Ivar do Sul, J.A., Shotyk, W., Turner, S., Wagreich, M., Zinke, J., 2021. The anthropocene: comparing its meaning in geology (chronostratigraphy) with conceptual approaches arising in other disciplines. *Earth's Future* 9, e2020EF001896. <https://doi.org/10.1029/2020EF001896>.
- Zeng, Y.L., Hao, D.L., Huete, A., Dechant, B., Berry, J., Chen, J.M., Joiner, J., Frankenberg, C., Bond-Lamberty, B., Ryu, Y., Xiao, J.F., Asrar, G.R., Chen, M., 2022. Optical vegetation indices for monitoring terrestrial ecosystems globally. *Nat. Rev. Earth Environ.* 3, 477–493. <https://doi.org/10.1038/s43017-022-00298-5>.
- Zhang, H.W., 2015. *Sediment Palynological Characteristic and its Environmental Significance in Semi-Humid and Semi-Arid Regions: Erlongshan Reservoir of Heilongjiang Province and Xiariburidu Lake of Inner Mongolia*. China University of Geosciences (in Chinese).
- Zhang, J., Huang, X.Z., Zhang, S.R., Ren, X.X., Xiao, Y.L., Wang, J.L., Xiang, L.X., Xu, Q.H., Birks, H.J.B., 2021. Cycles of grazing and agricultural activity during the historical period and its relationship with climatic and societal changes in northern China. *Land Degrad. Dev.* 32, 3315–3325. <https://doi.org/10.1002/lrd.4007>.
- Zhang, L.Y., 2009. *Pollen-Based Quantitative Reconstruction of about 600a Climate Changes in the Daihai Lake Area, Inner Mongolia, China*. Hebei Normal University, Shijiazhuang (in Chinese).
- Zhang, Q.H., Dong, X.H., Yang, X.D., Odgaard, B.V., Jeppesen, E., 2019. Hydrologic and anthropogenic influences on aquatic macrophyte development in a large, shallow lake in China. *Freshw. Biol.* 64, 799–812. <https://doi.org/10.1111/fwb.13263>.
- Zhang, Y.Q., Zhao, X., Gong, J., Luo, F., Pan, Y.P., 2024. Effectiveness and driving mechanism of ecological restoration efforts in China from 2009 to 2019. *Sci. Total Environ.* 910, 168676. <https://doi.org/10.1016/j.scitotenv.2023.168676>.
- Zhang, Z.J., Zhao, W.W., Liu, Y., Pereira, P., 2023a. Impacts of urbanisation on vegetation dynamics in Chinese cities. *Environ. Impact Assess. Rev.* 103, 107227. <https://doi.org/10.1016/j.eiar.2023.107227>.
- Zhang, Z.Y., Lu, L., Zhao, Y.H., Wang, Y.Y., Wei, D.D., Wu, X.D., Ma, X.L., 2023b. Recent advances in using Chinese Earth observation satellites for remote sensing of vegetation. *ISPRS J. Photogramm. Remote Sens.* 195, 393–407. <https://doi.org/10.1016/j.isprsjprs.2022.12.006>.
- Zhao, C., Guo, F., Zhao, Y.J., Xia, X.C., 2015. Pollen assemblages of *Tamarix* cone and environmental change in Andier ancient city region during the recent 200 years. *J. Arid Land Resour. Environ.* 29, 158–163. <https://doi.org/10.1344/j.cnki.jalre.2015.379> (in Chinese).
- Zhao, C.L., Yan, Y., Ma, W.Y., Shang, X., Chen, J.G., Rong, Y.J., Xie, T., Quan, Y., 2021. RESTREND-based assessment of factors affecting vegetation dynamics on the Mongolian Plateau. *Ecol. Model.* 440, 109415. <https://doi.org/10.1016/j.ecolmodel.2020.109415>.

- Zhao, L., Zeng, Y.Y., Rao, Z.G., Huang, C., Li, Y.X., Liu, L.D., Ma, C.M., 2024. Quantitative Holocene climate reconstruction and anthropogenic impact analysis based on the pollen records in peat sediment in Southern China. *Glob. Planet. Chang.* 234, 104390. <https://doi.org/10.1016/j.gloplacha.2024.104390>.
- Zhao, W.L., Xie, S.J., 1988. History of Population in China. People's Publishing House, Beijing (in Chinese).
- Zhao, Y., Yu, Z.C., Chen, F.H., Liu, X.J., Ito, E., 2008. Sensitive response of desert vegetation to moisture change based on a near-annual resolution pollen record from Gahai Lake in the Qaidam Basin, Northwest China. *Glob. Planet. Chang.* 62, 107–114. <https://doi.org/10.1016/j.gloplacha.2007.12.003>.
- Zhou, E.L., Liang, X., 1950. Directives on National Forestry Work by the Government Administration Council of the Central People's Government. Shanxi Zhengbao 6, 9–10 (in Chinese).
- Zhou, G.Y., Eisenhauer, N., Terrer, C., Eldridge, D.J., Duan, H.M., Guirado, E., Berdugo, M., Zhou, L.Y., Liu, S.G., Zhou, X.H., Delgado-Baquerizo, M., 2024. Resistance of ecosystem services to global change weakened by increasing number of environmental stressors. *Nat. Geosci.* 17, 882–888. <https://doi.org/10.1038/s41561-024-01518-x>.
- Zhou, R., 2014. Evolution of the Mangrove Coast and the Succession of Mangrove Community within the Last Hundred Years in Yingluo Bay, Guangxi province. East China Normal University, Shanghai (in Chinese).
- Zhou, S.F., Long, H., Xing, H., Zhang, K., Wang, R., Zhang, E.L., 2023a. Human activities facilitated the decline of forest ecosystem in East Asia after 5000 a BP. *Earth Sci. Rev.* 245, 104552. <https://doi.org/10.1016/j.earscirev.2023.104552>.
- Zhou, Y.H., Zhang, Y., Kong, Z.C., Yang, Z.J., Yan, Q.Y., 2023b. Vegetation changes and human activities in the *Betula* wetland of Habahe in Xinjiang, China since 3600 cal a BP. *Acta Ecol. Sin.* 43, 1156–1164. <https://doi.org/10.5846/stxb202110182930> (in Chinese).
- Zou, Y., Chen, W., Li, S.L., Wang, T.J., Yu, L., Zhang, X., Xu, M., Jiang, B.H., Wu, C.Y., Singh, R.P., Huete, A., Liu, C.Q., 2025. Assessing vegetation dynamics and human impacts in natural and urban areas of China: insights from remote sensing data. *J. Environ. Manag.* 373, 123632. <https://doi.org/10.1016/j.jenvman.2024.123632>.